The final publication is available at

https://doi.org/10.1177/1468087416678500

Additional Information

Evaluating the RCCI operating range limits in a high compression ratio medium-duty diesel engine fueled with biodiesel and ethanol

Jesús Benajes[1], Antonio García[1], Javier Monsalve-Serrano[1], Iyad Balloul[2] and Gérard Pradel[2]

[1]CMT – Motores Térmicos. Universitat Politècnica de València. Camino de Vera s/n, E-46022 Valencia, Spain.
[2]VOLVO Group Trucks Technology. 99 Route de Lyon, 69806 Saint Priest, France.

Corresponding author:
Name: A. García
E-mail: angarma8@mot.upv.es
Telephone: +(34) 963 876 574
Fax: +(34) 963 877 659

Abstract. This work investigates the load limits of reactivity controlled compression ignition (RCCI) combustion, a dual-fuel concept which combines port fuel injection of low reactivity fuels with direct injection of diesel fuel, in a medium-duty diesel engine. The experiments were conducted in a single-cylinder diesel engine derived from the multi-cylinder production engine. In this sense, the stock turbocharger and exhaust gas recirculation (EGR) systems were replaced by an external compressor and dedicated low pressure EGR loop, respectively. Additionally, a port fuel injector was installed in the intake manifold to allow gasoline injection. Firstly, the paper presents some results highlighting the effect of the EGR rate, gasoline fraction (GF), diesel start of injection (SOI), diesel injection strategy and intake temperature on the emissions, performance and combustion development in a representative operating condition; 1200 rpm and 6.5 bar IMEP (25% load). Later, with the aim of showing the RCCI potential, the best results in terms of performance and emissions at 25% load are compared against the multi-cylinder diesel engine from 950 to 2200 rpm. RCCI engine tests were developed taking into account limitations in nitrogen oxides (NOx) and soot emissions, in-cylinder pressure and maximum pressure rise rate. Finally, keeping the same constraints for testing, the load limits of RCCI concept are evaluated for all the engine speeds.

Results suggest that RCCI allows fulfilling EURO VI limits for NOx and soot emissions without using selective catalytic reduction (SCR) and diesel particulate filter (DPF) aftertreatment systems at 25% load at all engines speeds, providing better indicated efficiency than conventional diesel operation in most operating points. In addition, the maximum engine load that ensured the aforementioned constraints was around 35% for all engine speeds, with a maximum IMEP of 8.8 bar at 2200 rpm. In this case, a strong reduction in carbon monoxide (CO) and unburned hydrocarbons (HC) emissions compared to the cases of 25% load was achieved at all engine speeds.

Keywords: Reactivity controlled compression ignition; Dual-fuel combustion; EURO VI emissions; Efficiency; Biofuels

1. Introduction

As response of the regulations introduced around the world to limit the pollutant emissions associated to internal combustion engines, researchers and manufacturers are focusing their efforts on developing new combustion strategies and aftertreatment technologies to fulfill the stringent limitations imposed. Since the complex aftertreatment devices incur additional costs and fuel consumption, the emissions reduction from the in-cylinder standpoint is clearly necessary.

The more promising combustion strategies to improve the efficiency of compression ignition engines while reducing their most harmful emissions, NOx and soot, are the low temperature combustion (LTC) strategies. In this sense, homogeneous charge compression ignition (HCCI) has demonstrated great potential to inhibit the emission of these two pollutants while maintaining high efficiency [1][2]. However, great challenges regarding combustion control and mechanical engine stress were

identified [3]. Some researchers suggested that to achieve proper HCCI operation, the in-cylinder reactivity must vary depending on the operating conditions. These conditions could be achieved using high cetane fuels at low load and low cetane fuels at medium-high load [4]. With the aim of improving controllability and reduce the knocking level experienced during HCCI combustion, the use of gasoline-like fuels under partially premixed combustion (PPC) strategies has been widely studied [5][6][7]. These investigations confirmed gasoline PPC as promising method to control the heat release rate while providing a simultaneous reduction in NOx and soot emissions [8][9]. However, the concept demonstrated difficulties at low load conditions using gasoline with octane number (ON) greater than 90 [10][11]. At these conditions, the spark assistance provided temporal and spatial control over the gasoline PPC combustion process [12][13][14], but resulted in unacceptable NOx and soot emissions [15], even using double injection strategies [16][17].

More recently, experimental and computational studies proved that reactivity controlled compression ignition (RCCI), a dual-fuel LTC concept, has more potential than HCCI and PPC [18][19]. In particular, the gasoline fraction and the direct injection timing variation during RCCI operation [20][21] allow an effective control of the in-cylinder equivalence ratio and reactivity stratification [22][23] to promote the conditions necessary to achieve ultra-low NOx and soot emissions together with better fuel consumption than conventional diesel combustion (CDC) in a wide operating range of the engine [24].

In spite of the benefits obtained with RCCI concept, it was found that HC and CO emissions levels are considerably higher than CDC, mainly at low load operation. At these operating conditions, combustion efficiency values around 97% were observed. In this sense, it was demonstrated that these results can be improved up to values above 98% by combining the effects of in-cylinder gas temperature and oxygen concentration respectively with the in-cylinder fuel blending ratio [25]. Moreover, it was also confirmed that certain levels of unburned HC and CO remained unaffected in spite of the engine settings modification. This behaviour was previously identified to be consequence of the gasoline trapped in the crevice and squish volumes, which represents a primary source of incomplete combustion in RCCI combustion [26]. In addition, it was confirmed that RCCI concept also offers an interesting potential for improving fuel consumption by lowering wall heat transfer. Thus, with the aim of minimizing the unburned products and improve the indicated efficiency of the concept, the influence of piston geometry on RCCI combustion was also studied in literature [26]. In this case, it was found that a bathtub style piston with low surface area allowed a 2 to 4% absolute increase in gross indicated efficiency, which was attributed to both combustion efficiency and heat transfer improvement [27]. Some other geometries aimed at reducing the heat transfer losses were also tested, confirming that the best strategy to increase the efficiency of RCCI concept is by reducing the in-cylinder area-to-volume ratio [28][29]. However, these studies showed that an excessive shallow bowl combined with single injection strategies can result in unacceptable soot emissions when trying to extend the RCCI concept up to high loads.

Aside from the pollutant emissions, the internal combustion engines are responsible of near 60% of the energy consumption of petroleum products in Europe [30]. This data proves that, in addition to the need of developing advanced combustion strategies looking for high efficiency and ultra-low emissions, it is necessary that alternative fuels research be investigated in parallel to reduce the dependence on petroleum and minimize the environmental impact of transport sector. For this purpose, the Renewable Energy Directive (RED) establishes that all EU countries must ensure that at least 10% of their transport fuels come from renewable sources by 2020 [31]. Considering that the use of renewable liquid fuels would only demand a moderate evolution of both the vehicle technology and fuel distribution infrastructure, they are claimed as the most potential route to decarbonizing transportation.

Within the group of renewable liquid fuels, bioethanol and biodiesel have shown great potential as automotive fuels because they allow a successful reduction of engine-out emissions from conventional combustion processes, and can be made from a wide variety of feedstocks [32]. By these reasons, these two biofuels represent the most significant volume share in the future biofuels marketing scenarios considered to meet the 2020 target [20]. Thus, despite the maximum percentage currently allowed in the regular fuels in Europe is limited to 7% of biodiesel (in diesel) and 10% of ethanol (in gasoline) by volume [33], the use of higher blending ratios will be necessary to reach the objectives imposed by the RED.

Taking into account the key role that biofuels will play in road transport, the current research focuses on evaluating the operational limits of RCCI combustion in a medium-duty diesel engine, currently under serial production, by using biofuels which are expected to be near-term available in the fuel market in Europe. For this purpose, firstly, the main variables governing the RCCI combustion process are studied by means of parametric studies at 1200 rpm and 25% load. Later, a direct comparison between RCCI and conventional diesel combustion under original engine manufacturer (OEM) settings operation is presented at all the engine speeds. During the experimental tests, RCCI operation was considered acceptable only if it fulfilled several constraints simultaneously: NOx=0.4 g/kWh, soot=0.1

FSN, MPRR=15 bar/CAD and P_{max}=190 bar. These limits are aimed at ensuring ultra-low emissions while preserving the engine mechanical integrity. It is interesting to note that, although the maximum PRR limit proposed is higher than that experienced during conventional diesel combustion, 15 bar/CAD is typically used in literature to study this combustion mode and other LTC strategies in medium- and heavy-duty diesel engines.

2. Experimental facilities and processing tools

2.1 Test cell and engine description

The experiments presented in this work were conducted using a single-cylinder diesel engine (SCE) derived from the multi-cylinder production engine (MCE), whose main specifications are show in Table 1. As it can be seen, the engine used in this specific study is a EURO VI medium-duty diesel engine representative of urban freight distribution fleet.

Table 1. Main specifications of the medium-duty engine used in this study

Style	4 Stroke, DI diesel engine
Manufacturer / model	VOLVO / D5K240
OEM ECU calibration	EURO VI
Piston bowl geometry	Re-entrant
Maximum power	177 kW @ 2200 rpm
Maximum in-cylinder pressure	190 bar
Bore x Stroke	110 mm x 135 mm
Connecting rod length	212.5 mm
Crank length	67.5 mm
Total displaced volume	5100 cm^3
Number of cylinders	4
Compression ratio	17.5:1

The engine was installed in a fully instrumented test cell, with all the auxiliary facilities required for its operation and control, as it is illustrated in Figure 1. A particularity of the test cell set-up is that the engine used is not a conventional SCE research engine, but is a hybrid solution between a MCE and SCE. This engine configuration allows to study an isolated cylinder as conventional SCE engine, while the three remaining cylinders are governed using the OEM electronic control unit (ECU) to balance the cylinder-to-cylinder maximum pressure and load. This approach results in a much cheaper solution than the conventional SCEs used for research purposes, also allowing switching to the MCE version to broaden the spectrum of the study. However, as the crankshaft and the dynamometer are shared between both engine sides, it is not possible to obtain isolated torque-based parameters during the hybrid operation, which force to study the combustion process using indicated parameters. As expected, when switching to the MCE version, this limitation disappears.

As can be seen in Figure 1, the MCE side is also fully instrumented, which allows monitoring each subsystem during the engine operation. Thus, the in-cylinder pressure signals from both sides (SCE and MCE) are monitored in real-time for balancing purposes. In this sense, as the SCE conditions varied during the RCCI studies, the MCE settings were modified to provide similar maximum pressure, engine load and combustion phasing. Finally, it is interesting to note that as the MCE side of the engine is not used for studying the combustion process, the EGR rate was annulled to compensate part of the gas lost due to the isolated cylinder.
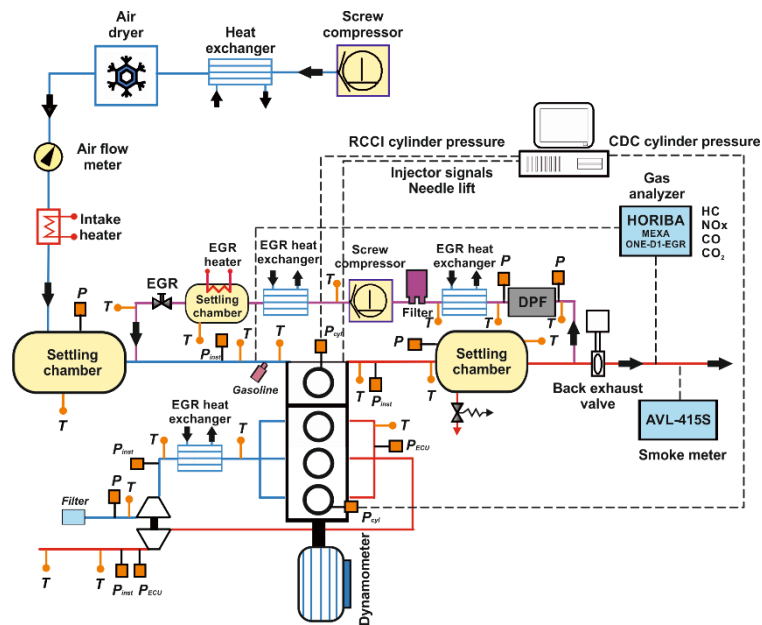
Figure 1. Test cell scheme showing the hybrid configuration. One cylinder is fully isolated and controlled by a full-pas driven controller. For balancing purposes, the three remaining cylinders operate under CDC conditions governed by the OEM ECU settings

From the test cell scheme shown in Figure 1, it can be seen that the main modifications done for isolating the cylinder in which the combustion study will be performed (from now on, SCE) are regarding air management. In particular, to achieve stable intake air conditions, a screw compressor supplied the required boost pressure before passing through an air dryer. The air pressure was adjusted within the intake settling chamber, while the intake temperature was controlled in the intake manifold after mixing with the EGR flow. The exhaust backpressure produced by the turbine in the real engine was replicated by means of a valve placed in the exhaust system, controlling the pressure in the exhaust settling chamber. Low pressure EGR was produced taking exhaust gases from the exhaust settling chamber. The determination of the EGR rate was carried out using the experimental measurement of intake and exhaust carbon dioxide (CO_2) concentration. The concentrations of NOx, CO, unburned HC, intake and exhaust CO_2, and oxygen (O_2) were analyzed with a five gas Horiba MEXA-ONE-D1-EGR analyzer bench by averaging 40 seconds after attaining steady state operation.

Smoke emission were measured with an AVL 415S Smoke Meter and averaged between three samples of a 1 liter volume each with paper-saving mode off, providing results directly in Filter Smoke Number (FSN) units. Finally, the in-cylinder pressure signal was measured with a Kistler 6125C pressure transducer coupled with a Kistler 5011B10 charge amplifier. A shaft encoder with 1800 pulses per revolution, which provides a resolution of 0.2 CAD, was used.

2.2 Fuels and delivery

Previous investigations developed by the authors showed the potential of biofuels for increasing the efficiency of RCCI concept [35]. These studies demonstrated that the combined use of biodiesel 7% (B7) as high reactivity fuel and an intermediate ethanol-gasoline blend as low reactivity fuel is a good strategy to find the proper reactivity gradient between both fuel sources [36]. In this sense, the relatively low ethanol quantity utilized allowed exploiting its unique characteristics (high octane number and enthalpy of vaporization) while minimizing some of the drawbacks related to using high ethanol fractions, such as high amount of HC and CO emissions, low thermal efficiency at low load and reduced volumetric fuel economy. Thus, gross indicated efficiencies higher than CDC, together with ultra-low NOx and soot emissions, were observed in a wide range of engine load-speed conditions [37].

Taking into account this experimental background, and considering the mandatory presence of biofuels in the future context of road transport, the low reactivity fuel (LRF) selected for performing this study was E20-95, a blend containing a nominal 20% ethanol and 95 ON gasoline. In addition, the high reactivity fuel (HRF) selected was diesel B7 as it showed good performance when combined with this intermediate ethanol-gasoline blend. Their main properties related to autoignition are listed in Table 2.

All the properties were obtained following the American Society for Testing and Materials (ASTM) standards. The characteristics of the regular European diesel fuel (EN590) are included in the table as this fuel was used for obtaining the results from CDC operation showed along the work.

Table 2. Physical and chemical properties of the fuels used along the study

	Diesel EN590	Diesel B7	E20-95
Density [kg/m^3] (T= 15 °C)	834.7	837.9	745
Viscosity [mm^2/s] (T= 40 °C)	2.55	2.67	-
RON [-]	-	-	99.1
MON [-]	-	-	85.6
Biodiesel content by volume [%]	<0.2	7	-
Ethanol content by volume [%]	-	-	19.7
Cetane number [-]	53	54	-
Lower heating value [MJ/kg]	42.97	42.61	40.05

To enable RCCI operation the engine was equipped with a double injection system, as it is shown in the scheme of Figure 2. This injection hardware enables to vary the in-cylinder fuel blending ratio and fuel mixture properties according to the engine operating conditions. For this purpose, the OEM ECU was replaced by a Drivven engine controller to allow full access for controlling the injection parameters of both direct injection (DI) and port fuel injector (PFI) systems.
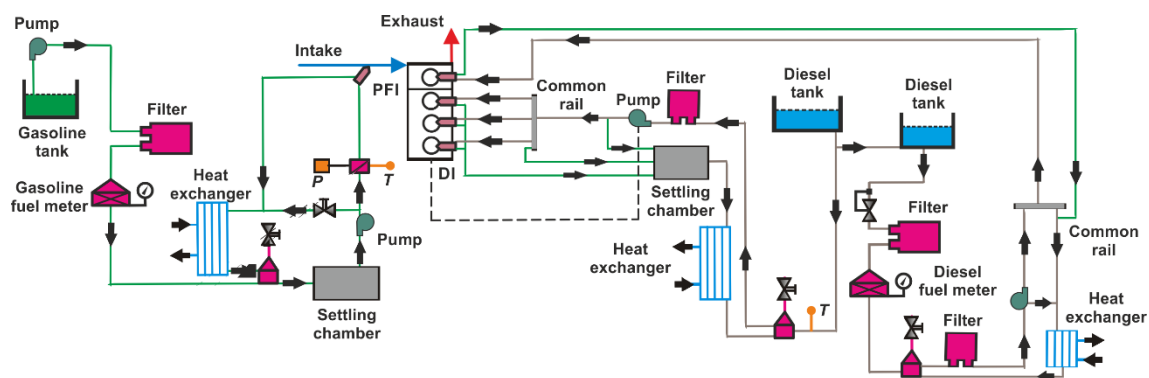

Figure 2. Fuel injection systems scheme

To inject the diesel fuel, the engine was equipped with a common-rail injection hardware [38][39][40]. Table 3 shows the main characteristics of the injector and nozzle used [41][42].

Table 3. Main characteristics of the high reactivity fuel injector

Actuation Type	Solenoid
Steady flow rate @ 100 bar [cm^3/min]	1300
Number of Holes	7
Hole diameter [μm]	177
Included Spray Angle [°]	150

Concerning the low reactivity fuel injection, an additional fuel circuit was in-house developed with reservoir, fuel filter, fuel meter, electrically driven pump, heat exchanger and a commercially available PFI. The mentioned injector was located at the intake manifold and was specified to be able to place all the low reactivity fuel into the cylinder during the intake stroke. Consequently, the injection timing was fixed 10 CAD after the intake valve opening (IVO) to allow the fuel to flow along the distance from the PFI location to the intake valves seats. Accordingly, this set up would avoid fuel pooling over the intake valve and the undesirable variability introduced by this phenomenon. The main characteristics of the port fuel injector are depicted in Table 4.

Table 4. Main characteristics of the high reactivity fuel injector

Injector Style	Saturated
Steady flow rate @ 3 bar [cm^3/min]	980
Included Spray Angle [°]	30
Injection Pressure [bar]	5.5
Injection Strategy	Single
Start of Injection Timing	340 CAD ATDC

2.3 In-cylinder pressure signal analysis

The combustion analysis was performed with an in-house one-zone model named CALMEC, which is fully described in [43]. This combustion diagnosis tool uses the in-cylinder pressure signal and some mean variables (engine speed, coolant, oil, inlet and exhaust temperatures, air, EGR and fuel mass flow…) as its main inputs.

The pressure traces from 150 consecutive engine cycles were recorded in order to compensate the cycle-to-cycle variation during engine operation. Thus, the individual pressure data of each engine cycle was smoothed using a Fourier series low-pass filter. Once filtered, the collected cycles were en-semble averaged to yield a representative cylinder pressure trace, which was used to perform the analysis. Then, the first law of thermodynamics was applied between intake valve closing (IVC) and exhaust valve opening (EVO), considering the combustion chamber as an open system because of the blow-by and fuel injection. The ideal gas equation of state was used to calculate the mean gas temperature in the chamber. In addition, the in-cylinder pressure signal allowed obtaining the gas thermodynamic conditions in the chamber to feed the convective and radiative heat transfer models [44], as well as the filling and emptying model that provided the fluid-dynamic conditions in the ports, and thus the heat transfer flows in these elements. The convective and radiative models are linked to a lumped conductance model to calculate the wall temperatures.

The main result of the model used in this work was the Rate of Heat Release (RoHR), the bulk gas temperature and the maximum pressure gradient in the combustion chamber. Moreover, several other parameters were calculated from the RoHR profile. In particular, the start of combustion (SOC) was defined as the crank angle position in which the cumulated heat release reached a value of 2% and combustion phasing was defined as the crank angle position of 50% fuel mass fraction burned (CA50).

3. Results and discussion

3.1 Effect of main variables governing RCCI combustion

The first campaign of RCCI tests performed in this new engine platform was aimed at acquiring knowledge about the engine response to modifications in the main variables governing the combustion process. In particular, the effects of EGR, gasoline fraction, diesel injection strategy and intake temperature were studied at a fixed engine speed of 1200 rpm and 25% load. Moreover, taking into account the great influence of the diesel injection timing on NOx and soot emissions [25], its effect was studied for each variable. The results from this study are presented next.

3.1.1 Effect of EGR rate

Figure 3 shows the indicated engine-out emissions for the tests corresponding to three different EGR rates (0%, 15% and 30%) and diesel injection timings varying from -60 to -25 CAD ATDC, in steps of 5 CAD. The intake temperature, intake pressure and gasoline fraction were held constant at 20°C, 1.5 bar and 86%, respectively. The total fuel mass delivered to the cylinder was 42 mg/cycle, which is the amount injected during CDC operation with OEM settings at this operating condition. Since the analysis is performed using indicated parameters, the EURO VI limits are included only as reference.
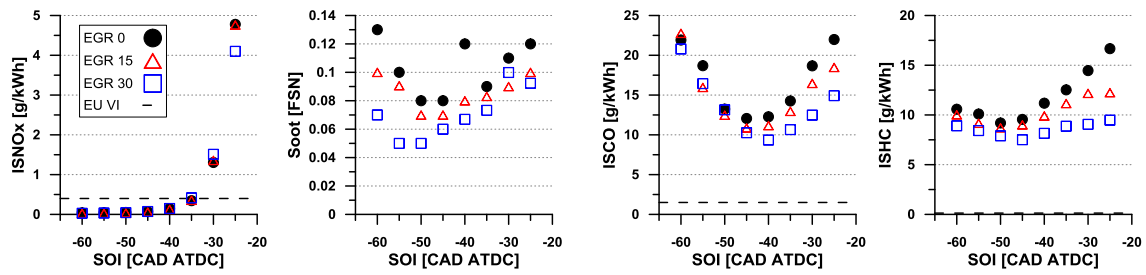
Figure 3. Indicated engine-out emissions results for different EGR rates and diesel injection timings at 1200 rpm and 25% load

As it can be seen, NOx emissions are unaffected by the EGR rate up to -35 CAD. In addition, the NOx levels are below the EURO VI limit in all these cases. The expected effect of EGR on NOx emissions is only observed at -25 CAD, where NOx are minimized when 30% EGR rate is used. However, no differences between 0% and 15% EGR are seen in all the SOI range.

The higher differences in soot emissions between the EGR rates are observed at the most advanced diesel injection timings. As diesel injection becomes more delayed than -40 CAD, soot emissions collapse to a common trend with similar values for the three EGR rates. This behavior is thought to be related with the higher mixing time available for the diesel fuel mass as EGR rate increases. This can be confirmed looking at the Figure 4, where the mixing time has been accounted as the period between the end of injection (EOI) and the SOC. As it is shown, up to -35 CAD, EGR 30% provides higher mixing time than the other two cases, which corresponds to the SOI range with the highest reductions in soot emissions. Later, mixing times become similar for the three EGR cases, and also do it their soot levels. On the other hand, soot emissions increase as SOI is delayed, which can be also explained by the trend of mixing time.
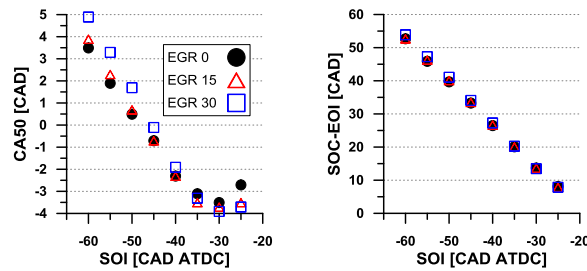

Figure 4. Combustion phasing (CA50) and mixing time (SOC-EOI) for different EGR rates and diesel injection timings at 1200 rpm and 25% load

Carbon monoxide (CO) and unburned hydrocarbons (HC) show the same trend between EGR cases as SOI varies. From -60 to -35 CAD, CO levels are almost equal for all the EGR cases. This fact suggests that the maximum in-cylinder temperatures must be similar. This would also explain the similarities in NOx emissions in this SOI range. After -35 CAD, the CO levels are notably lower for the higher EGR rates. Hydrocarbons emissions present the same trend than CO, but show a slightly higher sensitivity to the EGR rate in the advanced SOI range. The reduction in both emissions indicates that combustion development is enhanced as EGR increases, which suggests that higher EGR rates promote richer equivalence ratios and minimize over-mixing conditions. This can be confirmed looking at the RoHR profiles of the most delayed diesel SOIs shown in Figure 5. From this figure, it is also interesting to see how the RoHR profiles transition from Gaussian-shaped to u-shaped as SOI is retarded, as has been already identified in previous works [29][36].

From the figure it is possible to state that, at the most advanced injection timing (-60 CAD), the RoHR becomes smoother and delayed (see CA50 in Figure 4) as EGR increases. Delaying the diesel SOI up to -35 CAD, the benefits of EGR on combustion development appear. As EGR is increased from 0% to 15%, the late soft burning period is reduced with equal RoHR development up to top dead center (TDC). Further increase in EGR rate up to 30% improves both the maximum RoHR peak and the expansion period, which explain the lower HC and CO emissions in this case. At -25 CAD, it is clearly seen that the increase in EGR enhances the second combustion stage, where the majority of LRF is burned, while the first one remains almost unaffected. This improvement of the LRF burning explains the great reduction of unburned HC observed in Figure 3.
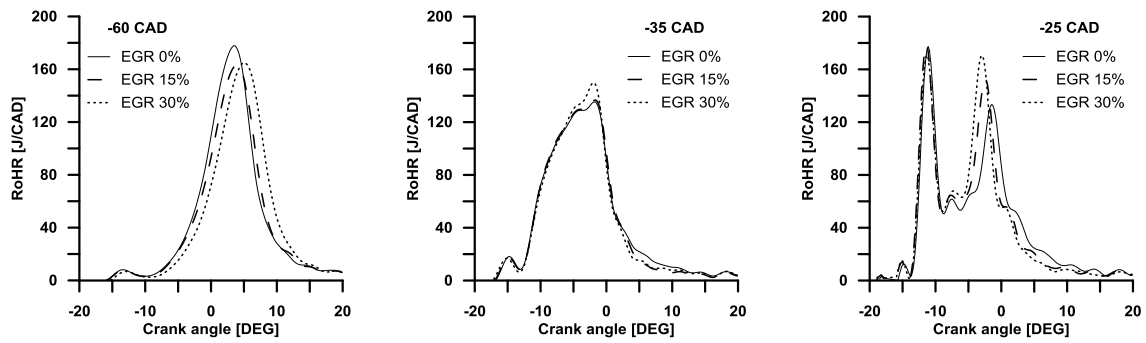
Figure 5. RoHR profiles for three injection timings (-60, -35 and -25 CAD) and EGR rates of 0%, 15% and 30%

Lastly, Figure 6 shows the performance results obtained in this batch of tests. As can be seen, the gross indicated efficiency (GIE) follows the same trend than CO and HC (combustion efficiency), showing minor differences between the three cases from -60 to -35 CAD. For more delayed SOI values, the combustion enhancement as EGR increases results in higher IMEP and therefore higher GIE.

Regarding the in-cylinder pressure limitations, the figure shows that EGR 30% allows a reduction in maximum pressure of around 15 bar in average. The maximum pressure rise rates at delayed SOIs remain unaffected as EGR varies, and shows greater influence as SOI is advanced. This trend agrees with Figure 4, which shows that the EGR increase retards the combustion phasing (CA50) at early SOIs.
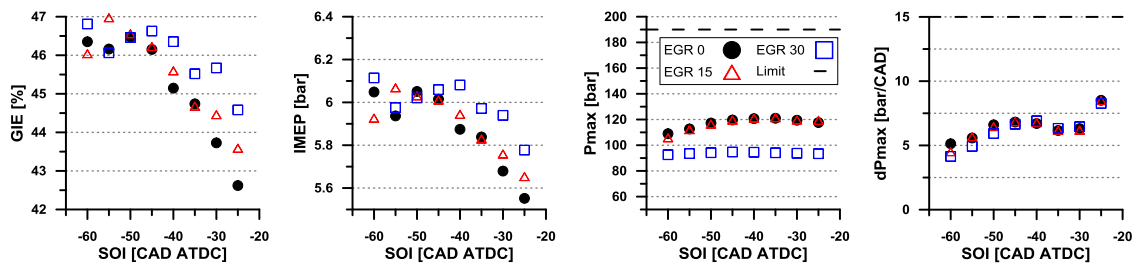

Figure 6. Performance results for different EGR rates and diesel injection timings at 1200 rpm and 25% load

3.1.2 Effect of gasoline fraction

Figure 7 shows the indicated engine-out emissions for two GF conditions (76% and 86%), defined as the ratio of gasoline to total fuel mass, and diesel injection timings varying from -60 to -25 CAD ATDC, in steps of 5 CAD. The intake temperature and intake pressure were held constant at 20°C and 1.5 bar. The EGR rate was fixed at 30% as it showed the best results in the previous section, and the total fuel injected was 42 mg/cycle.
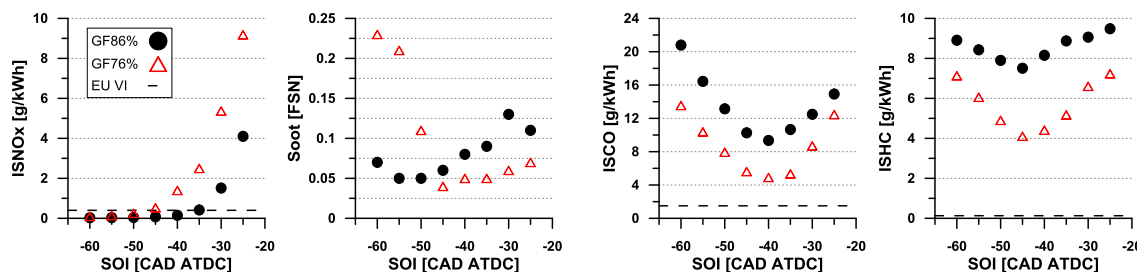

Figure 7. Indicated engine-out emissions results for different gasoline fractions and diesel injection timings at 1200 rpm and 25% load

The figure shows that, for both GF cases, NOx emissions increase as diesel SOI is delayed towards TDC. This behavior is related to the shifting of the combustion event towards the compression stroke (see Figure 8). Moreover, it is clear that the increase in GF allows a notable reduction in NOx levels, allowing the EURO VI compliance in greater number of tests. This reduction is achieved due to the more delayed CA50, which minimizes the portion of the combustion event that evolves during the compression stroke and causes the thermal NOx formation.

The trend of soot emissions varies notably depending on the GF used. In particular, GF 86% shows a constant increase in soot emissions as diesel injection timings move towards TDC, while GF 76% only shows this trend for diesel SOIs more delayed than -50 CAD. Thus, this GF promotes high soot emissions for the early injection timings, then showing a rapid fall in soot levels as the diesel SOI delays up to -45 CAD. As can be seen in Figure 8, the mixing time shows a constant decay as diesel SOI is delay. Thus, the trend of soot emission at the early SOI timings must be governed by some local phenomenon.

As expected, CO and HC levels increase considerably as GF increases. As it can be seen, CO emissions show the same u-shaped trend in both GF scenarios, which follows an inverse trend than the bulk gas temperature peak (Figure 8). However, HC emissions are less sensitive to diesel SOI modification in the case of the highest GF. This is thought to be related with the higher amount of gasoline trapped in the crevice region.
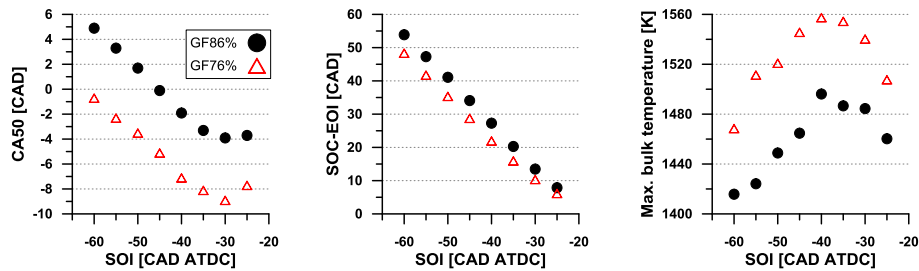

Figure 8. Combustion phasing (CA50), mixing time (SOC-EOI) and maximum bulk gas temperature for different gasoline fractions and diesel injection timings at 1200 rpm and 25% load

Regarding engine performance, shown in Figure 9, it is seen that the retarded combustion phasing obtained by the increase in GF leads to higher IMEP and GIE values in all the SOI range tested. Moreover, the maximum in-cylinder pressure is reduced for the most advanced diesel SOIs, which can be also observed in Figure 10. Finally, an almost constant reduction in maximum pressure rise rate (MPRR) of around 2.5 bar is observed for the tests with higher GF. The sudden increase in the MPRR at the most delayed SOIs is related to the change in the heat release shape, which moves from a one-staged to a two-staged heat release. Thus, as SOI is delayed, the mixing time gets shorter (Figure 8), which promotes richer equivalence ratio distributions for the diesel fuel and enhances the first combustion stage.
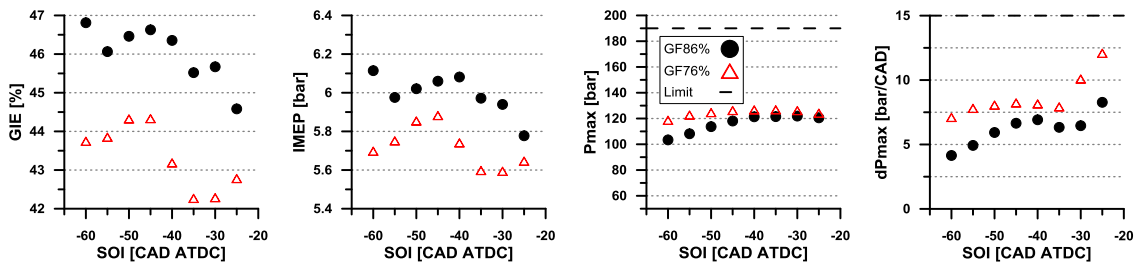

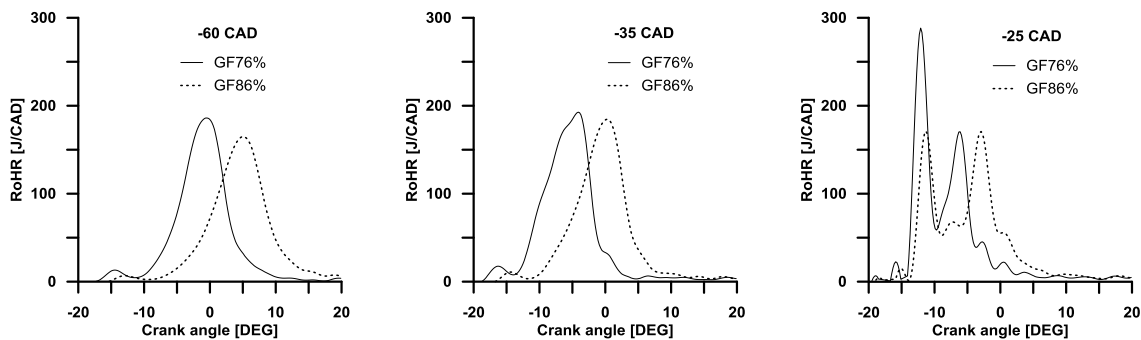**Figure 9.** Performance results for different gasoline fractions and diesel injection timings at 1200 rpm and 25% load

Figure 10. RoHR profiles for three injection timings (-60, -35 and -25 CAD) and GF of 76% and 86%

3.1.3 Effect of diesel injection strategy

Figure 11 shows the indicated engine-out emissions for two diesel injection strategies, single and double. In the case of single injection, the diesel timings were varied from -60 to -25 CAD ATDC in steps of 5 CAD. In the case of double injection, the pilot event was fixed at -50 CAD and the main injection was swept from –45 to 0 CAD TDC in steps of 5 CAD. The fuel mass was split to 50% between both injection events considering the results of a previous dedicated study. For the shake of brevity, these results are not shown here, but the effects of this injection parameter on RCCI combustion can be found in [45]. For this study, the intake temperature and intake pressure were held constant at 20°C and 1.5 bar. The EGR rate was fixed at 30% and the GF at 86%, as these values showed the best results in previous sections. The total fuel injected was 42 mg/cycle.
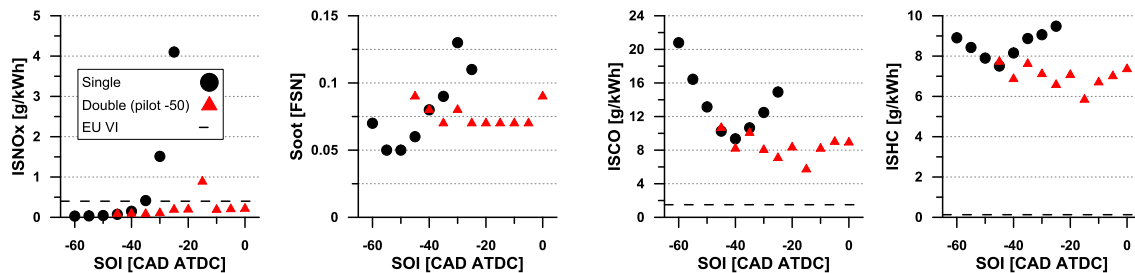

Figure 11. Indicated engine-out emissions results for different diesel injection strategies and timings at 1200 rpm and 25% load

Focusing on NOx emissions, it is seen that the double injection strategy allows achieving the EURO VI limit in almost all the SOI range of the main diesel injection. Only a singular test is identified at -50/-15 CAD TDC, in which the NOx emissions exceed 0.4 g/kWh. Comparing the soot emissions levels of the single injection at -50 CAD ATDC with the ones corresponding to double injection, it can be seen that the latter strategy leads to higher levels in all cases. This can be explained due to the reduction of the mixing time for the portion of fuel mass corresponding to the main injection, which promotes richer equivalence ratio distributions at the autoignition time [36]. As can be seen in Figure 12, the portion of the fuel injected in the pilot event shows an almost equal mixing time. However, it is interesting to note that all cases provide ultra-low soot levels, being below the limit of 0.1 FSN imposed in the study. Finally, as Figure 12 shows, the use of a main injection provokes an increase in the in-cylinder bulk temperature, which leads to reduce the CO and HC emissions if compared with the single injection strategy at -50 CAD. It is interesting to note that, in spite of that the bulk temperature is increased with double injection, the decrease in overall stratification likely results in lower local peak equivalence ratio and reactivity at the time of ignition, which would then result in lower local peak temperatures. This line of reasoning is supported by the NOx results, which are much lower with double injection despite the increase in bulk temperature.
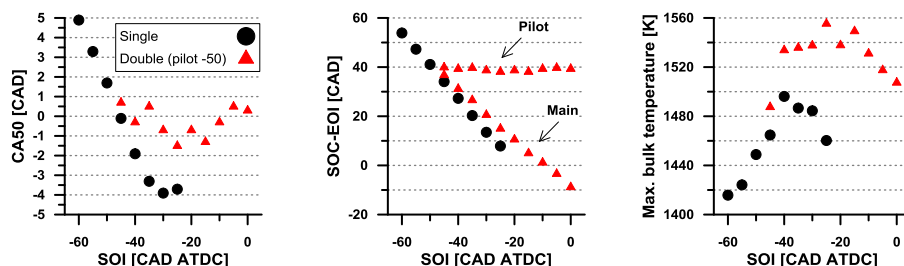

Figure 12. Combustion phasing (CA50), mixing time (SOC-EOI) and maximum bulk gas temperature for single and double injection strategies with different diesel injection timings at 1200 rpm and 25% load

Figure 13 shows that the double injection strategy can allow to increase the GIE versus the single strategy set at -50 CAD ATDC. This improvement is consequence of the higher IMEP, which is explained due to slight differences in the combustion cycle (CA50 and maximum heat release rate). In addition, the better combustion efficiency (lower CO and HC) also contributes to increase the IMEP. Finally, it is seen that the maximum in-cylinder pressure and the maximum pressure rise rate are very similar for both injection strategies.
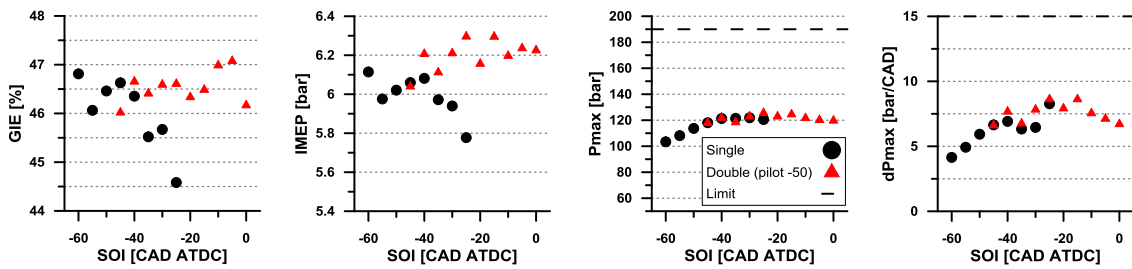
Figure 13. Performance results for different diesel injection strategies and timings at 1200 rpm and 25% load

3.1.4 Effect of intake temperature

The last parameter analyzed is the intake temperature. For this purpose, the Figure 14 depicts the same results than in the previous section (filled symbols) together with new results obtained with intake temperature of 38°C (empty symbols). With the new temperature, more representative of real engine conditions, the diesel SOI was swept from –60 to –30 CAD TDC in steps of 10 CAD in the case of single injection, and from –15 to 0 CAD TDC in steps of 5 CAD in the case of double injection. The rest of engine settings were equal than those used in the previous section.
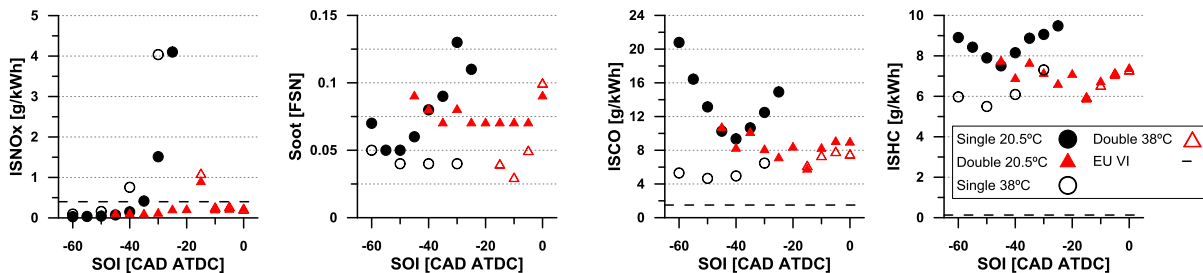

Figure 14. Indicated engine-out emissions results for different intake temperatures and diesel injection timings at 1200 rpm and 25% load. Single and double injection strategies are evaluated

As expected, the intake temperature increase provokes an increase in NOx emissions, but this effect is only observed when single injections are used. Moreover, at the most advanced diesel SOIs, the increase in NOx emissions is insignificant. The figure also shows that, for the double injection cases, the intake temperature increase does not have an appreciable effect on NOx emissions. This suggests that the combustion development is not greatly affected, which can be confirmed looking at Figure 15, where similar values of CA50 and maximum bulk gas temperature are seen for both intake temperatures. On the other hand, it is seen that soot emissions decrease as temperature increases for both injection strategies. Considering that the mixing time remains almost unaffected (see Figure 15), this behavior should be explained by the improving of the soot oxidation process.

In the case of single injection, the increase in temperature implies great reduction of both CO and HC emissions. Comparing the reduction experienced in both pollutants, it is confirmed again the higher sensitivity to the temperature of CO than HC. The bulk gas temperature peak in the case of double injection does not show much increase in the case of Tintake=38°C, which explains the low reduction observed in CO emissions. Moreover, the hydrocarbon emissions remain at the same levels than in the cases of 20.5°C.
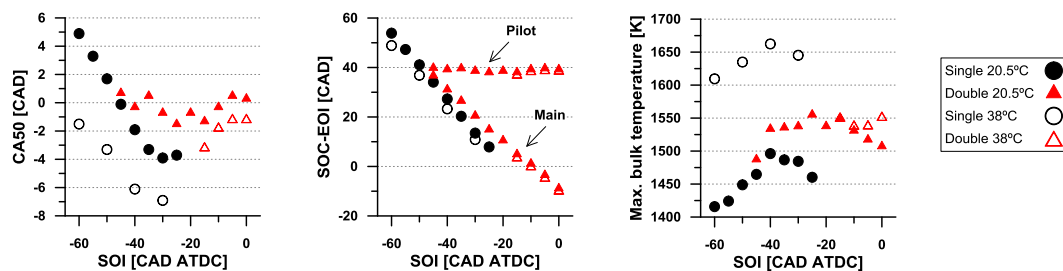

Figure 15. Combustion phasing (CA50), mixing time (SOC-EOI) and maximum bulk gas temperature for two intake temperatures with different diesel injection timings at 1200 rpm and 25% load

The performance results shown in Figure 16 indicate that the increase of the intake temperature leads to worsen engine performance. The GIE decrease is directly related with the reduction of the IMEP, which is explained by the shifting of the combustion development towards the compression stroke (see CA50 in Figure 15). Nonetheless, it is expected that this efficiency penalty can be reduced by managing the engine settings to achieve a proper combustion phasing. Moreover, it is seen that the intake temperature increase causes an increase in both maximum in-cylinder pressure and maximum pressure rise rate in the case of single injection. In the case of double injection, the maximum in-cylinder pressure remains equal for both intake temperatures.
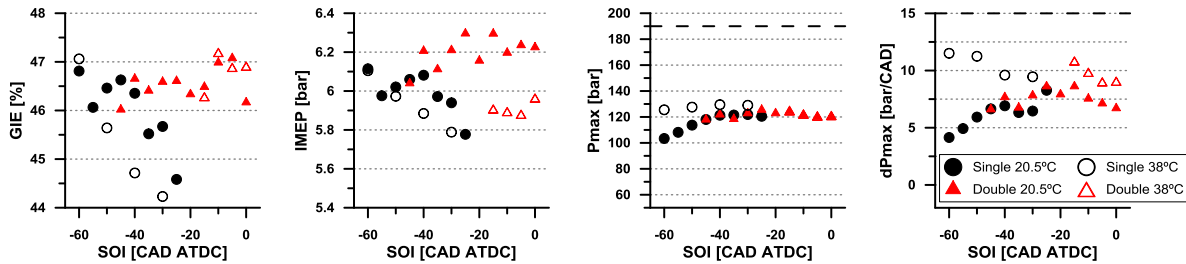

Figure 16. Performance results for different intake temperatures and diesel injection timings at 1200 rpm and 25% load. Single and double injection strategies are evaluated

3.2 Engine operational limits working under RCCI regime

After performing the parametric sweeps, a similar experimental procedure to the one described in [37] was carried out. The constrained values in this case were NOx=0.4 g/kWh, soot=0.1 FSN, MPRR=15 bar/CAD and P_{max}=190 bar. The intake temperature was fixed at 38°C because it allowed operating under the constraints proposed and moreover reproduces more realistic engine conditions than 20°C.

The direct comparison between the emissions and performance of RCCI and CDC at 25% load is shown in Figure 17. In addition, the results corresponding to the maximum load achievable under RCCI conditions considering the different constraints are depicted in the figure. Again, it is interesting to remark that the EURO VI limits are included in the different subfigures only as reference.
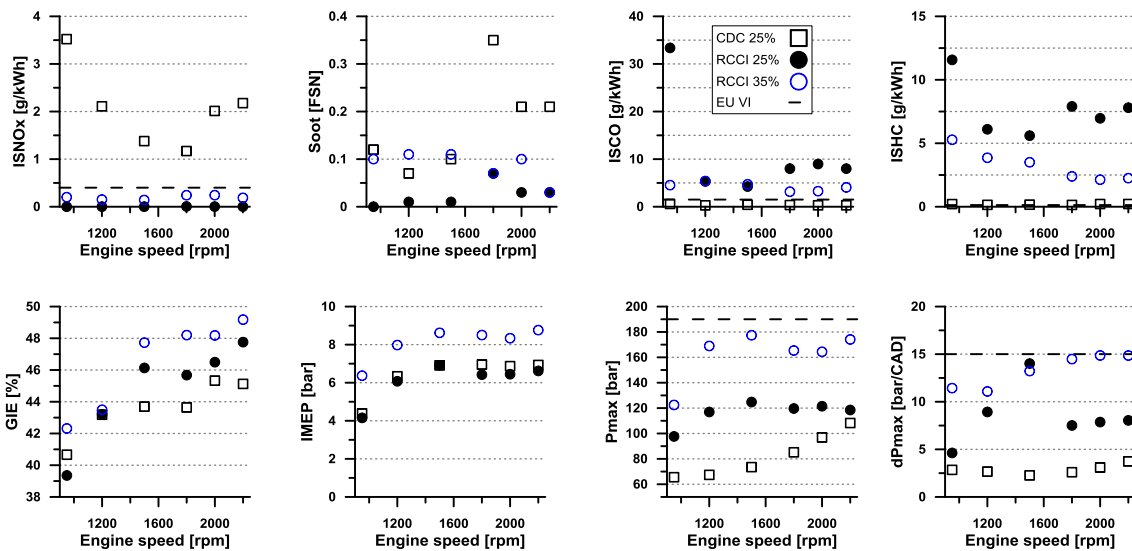

Figure 17. Comparison of emissions and performance between RCCI and CDC at 25% load at different engine speeds. The results from RCCI at 35% load are also included

Comparing the results at 25% load for both operating modes, it is demonstrated again the ability of RCCI to avoid the classical NOx-soot trade-off, providing a simultaneous reduction of both emissions up to values under the limits imposed. The higher benefits of RCCI versus CDC are observed in NOx emissions, while the major improvements in soot emissions are observed at high engine speeds. This fact is related with the CDC calibration used in the production engine. As expected, RCCI combustion results in higher CO and HC emissions than CDC, but it is interesting to see that these levels are quite lower than those obtained in previous work using a heavy-duty engine with lower compression ratio [37].

Regarding engine performance, it can be seen that RCCI provides higher GIE than CDC at medium-high engine speeds (1500 and 2200 rpm) and the benefits become unclear at lower engine speeds (950 and 1200 rpm). This was mainly consequence of the poor combustion efficiency, as it is inferred looking at the HC and CO emissions subfigures. Finally, it is seen that the maximum in-cylinder pressures under RCCI regime were below the limit imposed of 190 bar, and only one test at 1500 rpm was near the maximum PRR limitation.

Focusing on the RCCI results at maximum load, it is seen that the greater value feasible working under the imposed constraints was 35% at all the engine speeds. As it can be seen, the high values of PRR and P_{max} were found as the limiting factors to further increase the maximum operable load. The comparison of RCCI emissions results between 25% and 35% load reveals a great reduction in CO and HC emissions as load increases, providing CO levels near the EURO VI limits in some cases. In addition, at maximum load, NOx emissions were below the limitations imposed and soot levels were just in the limit value.

Figure 18 summarizes the main engine settings used to reach the previous RCCI results. At 25% load, the average GF used was 85% with a peak of 95% at 1500 rpm. The majority of tests at this load were obtained using a combination of an advanced pilot injection and a main injection near TDC. In some conditions, this was found an effective strategy to reduce HC and CO emissions due to the better diesel fuel stratification. At 35% RCCI operation, the GF was reduced around 5% in average compared to 25% load results to avoid the increasing knocking tendency, but the trends observed in this parameter versus the engine speed were very similar in both cases. At this load, the RCCI operation was achieved through an early single pulse of diesel fuel between -45 and -70 CAD ATDC in all the cases. The diesel SOI was advanced as engine speed increases to compensate the lower duration of the engine cycle.

Finally, it is seen that the EGR and intake pressure levels used in all the cases are representative of those used in the OEM calibration for CDC operation. Moreover, the diesel injection pressure was fixed at 1000 bar to minimize the variables included in the experimental procedure. However, in one operating condition it was necessary to increase this value up to 1300 bar to reduce soot emissions below the limit of 0.1 FSN.
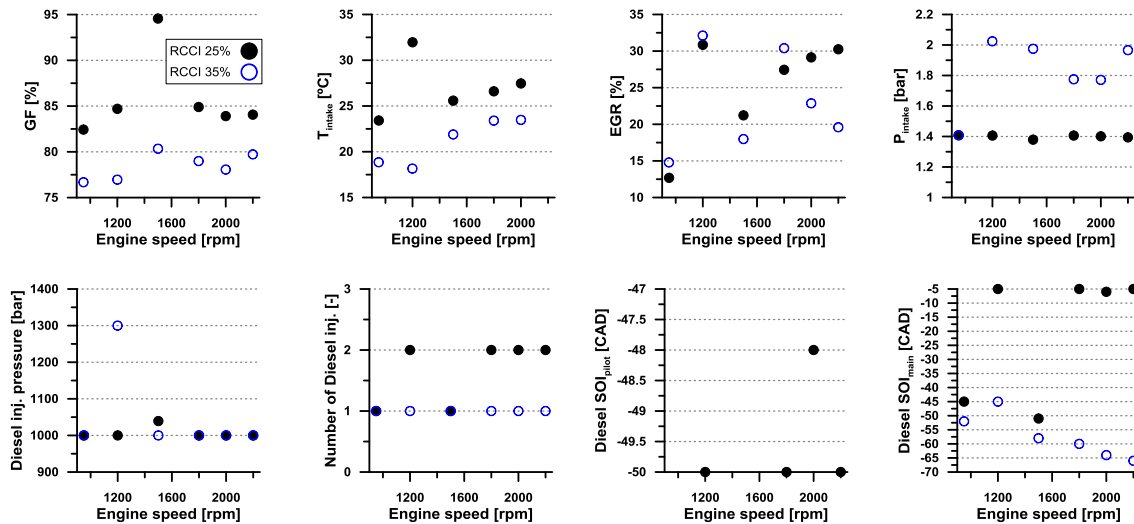

Figure 18. Comparison of the engine settings used to obtain the RCCI results at 25% and 35% load at different engine speeds

4. Conclusions

The present work has investigated the operating limits of RCCI combustion in a high compression ratio medium-duty diesel engine using biofuels. For this purpose, a batch of experiments aimed at capturing the influence of the main variables governing RCCI combustion on performance and emissions, was done first. The major findings from this particular study are summarized as follows:

- Under the operating conditions proposed, high EGR reduces over-dilution and enhances the combustion process. This reduces HC and CO notably and increases the gross indicated efficiency. For delayed SOIs, the increase in EGR promotes better gasoline burning, which was observed as improvement in the second stage of the RoHR.

- The increase in gasoline fraction entails a reduction in NOx levels with considerably increase in HC and CO emissions. CO emissions are found to be more sensitive to diesel SOI variation than HC, following the in-cylinder peak temperature. The low sensitivity of HC with high gasoline fractions is thought to be related with the greater amount of gasoline trapped in crevice regions.

- The use of double injection strategy leads to increase the in-cylinder temperature, which reduces considerably CO and HC emissions. NOx emissions were not affected by the increase in temperature, which remained under the EURO VI limits. Soot emissions increased slightly because of the shorter mixing time for the main injection, but the engine-out levels were far below the limit imposed (below 0.1 FSN). In addition, the slight differences in CA50 and the higher RoHR peaks resulted in greater IMEP and GIE than single injection.

- The effect of intake temperature was more noticeable in the case of single injection strategy. In particular, it was seen that the intake temperature increase led to greater NOx with lower soot, CO and HC emissions. In addition, the enhancement of the combustion process resulted in higher maximum in-cylinder pressures and greater pressure rise rates. The higher intake temperature provoked also a slight decrease of GIE due to the shifting of the CA50 towards the compression stroke.

Later, the comparison of the RCCI and CDC results at 25% load showed that RCCI allows avoiding the classical NOx-soot trade-off experienced during CDC operation, which provides a simultaneous reduction of both emissions up to values under the limits imposed. Moreover, it was confirmed that RCCI provides higher GIE than CDC at medium-high engine speeds and worse efficiency than CDC at 950 rpm due to the low combustion efficiency. Since NOx and soot emissions remained near-zero levels at these operating points, future works could improve this results by decreasing the gasoline fraction at these conditions.

Considering the next constraints: NOx=0.4 g/kWh, soot=0.1 FSN, MPRR=15 bar/CAD and P_{max}=190 bar, it was found that the maximum operable load under RCCI conditions was 35% at all engine speeds. At these conditions, the in-cylinder peak pressure and the maximum pressure rise rate were identified as limiting factors. In addition, soot levels were also near the limit proposed. By contrast, NOx emissions were still far below the EURO VI limit.

Finally, it should be noted that this was a first attempt at evaluating the RCCI operation in a high compression ratio diesel engine. The results presented here are primarily intended to provide guidance to get stable RCCI operation under certain constraints and therefore have not been rigorously optimized. Therefore, it is expected that different combinations of engine settings may yield similar or even better results. Taking into account the conclusions of the present work, further studies are currently underway to investigate the capabilities of the dual-mode RCCI/CDC operation to cover all the operating range of the engine.

Declaration of conflicting interests

The authors declared no potential conflicts of interest with respect to the research, authorship, and/or publication of this article.

Acknowledgments

Funding

References

[1] Mingfa Y, Zhaolei Z and Haifeng L. Progress and recent trends in homogeneous charge compression ignition (HCCI) engines. Progress in Energy and Combustion Science, Vol.35 (5), pp. 398-437, 2009.

[2] Maurya RK and Agarwal AK. Experimental study of combustion and emission characteristics of ethanol fuelled port injected homogeneous charge compression ignition (HCCI) combustion engine. Applied Energy, Vol. 88, pp 1169-1180, 2011.

[3] Cerit M and Soyhan HS. Thermal analysis of a combustion chamber surrounded by deposits in an HCCI engine. Applied Thermal Engineering 50 (1) (2013) 81-88.

[4] Bessonette PW, Schleyer CH, Duffy KP, Hardy WL and Liechty MP. Effects of fuel property changes on heavy-duty HCCI combustion. SAE paper 2007-01-0191, 2007.

[5] Singh AP and Agarwal AK. Combustion characteristics of diesel HCCI engine: an experimental investigation using external mixture formation technique. Appl Energy 2012. Vol. 99, pp. 116-125, 2012.

[6] Haraldsson G, Tunestål P, Johansson B and Hyvönen J. HCCI combustion phasing in a multi cylinder engine using variable compression ratio. SAE paper 2002-01-2858; 2002.

[7] Maurya RK and Agarwal AK. Experimental investigation on the effect of intake air temperature and air–fuel ratio on cycle-to-cycle variations of HCCI combustion and performance parameters. Applied Energy, Vol. 88, pp 1153-1163, 2011.

[8] Kalghatgi GT. Auto-ignition quality of practical fuels and implications for fuel requirements of future SI and HCCI engines. SAE paper 2005-01-0239, 2005.

[9] Kalghatgi G, Risberg P and Angstrom H. Advantages of fuels with high resistance to autoignition in late-injection, low-temperature, compression ignition combustion. SAE Trans., 2006, 115(4), 623–634.

[10] Liu H, Yao M, Zhang B and Zheng Z. Effects of inlet pressure and octane numbers on combustion and emissions of a homogeneous charge compression ignition (HCCI) engine. Energy and Fuels, 2008, 22(4), 2207–2215.

[11] Christensen M, Hultqvist A and Johansson B. Demonstrating the multi-fuel capability of a homogeneous charge compression ignition engine with variable compression ratio. SAE paper 1999-01-3679, 1999.

[12] Benajes J, García A, Domenech V and Durrett R. An investigation of partially premixed compression ignition combustion using gasoline and spark assistance. Applied Thermal Engineering, Volume 52, Issue 2, 15 April 2013, Pages 468-477.

[13] Benajes J, García A, Tormos B and Monsalve-Serrano J. Impact of Spark Assistance and Multiple Injections on Gasoline PPC Light Load. SAE Int. J. Engines 7(4):2014, doi:10.4271/2014-01-2669.

[14] Pastor JV, García-Oliver JM, García A, Micó C and Durrett R. A spectroscopy study of gasoline partially 365 premixed compression ignition spark assisted combustion. Appl Energy 2013;104:568–75. 366.

[15] Desantes JM, Payri R, García A and Monsalve Serrano J. Evaluation of Emissions and Performances from Partially Premixed Compression Ignition Combustion using Gasoline and Spark Assistance. SAE Technical Paper 2013-01-1664, 2013, doi:10.4271/2013-01-1664.

[16] Benajes J, Molina S, García A, Monsalve-Serrano J and Durrett R. Conceptual model description of the double injection strategy applied to the gasoline partially premixed compression ignition combustion concept with spark assistance. Applied Energy, Vol. 129, 15 September 2014, Pages 1-9.

[17] Benajes J, Molina S, García A, Monsalve-Serrano J and Durrett R. Performance and engine-out emissions evaluation of the double injection strategy applied to the gasoline partially premixed compression ignition spark assisted combustion concept. Applied Energy, Vol. 134, pp. 90-101, 2014.

[18] Splitter DA, Wissink ML, Hendricks TL, Ghandhi JB and Reitz RD. Comparison of RCCI, HCCI, and CDC Operation from Low to Full Load, THIESEL 2012 Conference on Thermo- and Fluid Dynamic Processes in Direct Injection Engines, 2012.

[19] Kokjohn S, Hanson R, Splitter D and Reitz, R. Experiments and Modeling of Dual-Fuel HCCI and PCCI Combustion Using In-Cylinder Fuel Blending. SAE Int. J. Engines 2(2):24-39, 2010, doi:10.4271/2009-01-2647.

[20] Kampman B, Verbeek R, van Grinsven A, van Mensch P, Croezen H and Patuleia A. Bringing bio-fuels on the market: options to increase EU biofuels volumes beyond the current blending limits. CE Delft, 2013.

[21] Klos D, Janecek D and Kokjohn S. Investigation of the Combustion Instability-NOx Tradeoff in a Dual Fuel Reactivity Controlled Compression Ignition (RCCI) Engine. SAE Int. J. Engines 8(2):2015, doi:10.4271/2015-01-0841.

[22] Kokjohn S, Musculus M and Reitz R. Evaluating temperature and fuel stratification for heat-release rate control in a reactivity-controlled compression-ignition engine using optical diagnostics and chemical kinetics modeling. Combustion and Flame, 162 (2015) 2729–2742.

[23] Kokjohn S, Reitz R, Splitter D and Musculus M. Investigation of Fuel Reactivity Stratification for Controlling PCI Heat-Release Rates Using High-Speed Chemiluminescence Imaging and Fuel Tracer Fluorescence. SAE Int.J. Engines 5(2):2012, doi:10.4271/2012-01-0375.

[24] Kokjohn SL, Hanson RM, Splitter DA and Reitz RD. Fuel reactivity controlled compression ignition (RCCI): a pathway to controlled high-efficiency clean combustion, International Journal of Engine Research, 2011. Volume 12, June 2011, Pages 209-226.

[25] Desantes JM, Benajes J, García A and Monsalve-Serrano J. The Role of the In-Cylinder Gas Temperature and Oxygen Concentration over Low Load RCCI Combustion Efficiency. Energy, Volume 78, 15 December 2014, Pages 854–868.

[26] Splitter DA, Kokjohn SL, Wissink ML and Reitz R. Effect of compression ratio and piston geometry on RCCI load limits and efficiency. SAE technical paper 2012-01-0383; 2012.

[27] Dempsey A, Walker N and Reitz R. Effect of Piston Bowl Geometry on Dual Fuel Reactivity Controlled Compression Ignition (RCCI) in a Light-Duty Engine Operated with Gasoline/Diesel and Methanol/Diesel. SAE Int. J. Engines 6(1):78-100, 2013, doi:10.4271/2013-01-0264.

[28] Benajes J, García A, Pastor JM and Monsalve-Serrano J. Effects of piston bowl geometry on Reactivity Controlled Compression Ignition heat transfer and combustion losses at different engine loads. Energy, Volume 98, 1 March 2016, Pages 64-77.

[29] Benajes J, Pastor JV, García A and Monsalve-Serrano J. An experimental investigation on the Influence of piston bowl geometry on RCCI performance and emissions in a heavy-duty engine. Energy Conversion and Management, Volume 103, October 2015, Pages 1019-1030.

[30] The European Commission. Energy, Transport and Environment Indicators. Publications Office of the European Union, 2014.

[31] Directive 2009/28/EC of the European parliament and of the council of 23 April 2009 on the promotion of the use of energy from renewable sources. http://eur-lex.europa.eu.

[32] Pearson RJ and Turner JW. The role of alternative and renewable liquid fuels in environmentally sustainable transport. Alternative Fuels and Advanced Vehicle Technologies for Improved Environmental Performance, 2014, Pages 19–51.

[33] Directive 2009/30/EC of the European parliament and of the council of 23 April 2009. http://eur-lex.europa.eu.

[34] Yu S and Zheng M. Ethanol–diesel premixed charge compression ignition to achieve clean combustion under high loads. Proceedings of the Institution of Mechanical Engineers, Part D: Journal of Automobile Engineering, 2015. doi: 10.1177/0954407015589870.

[35] Benajes J, Molina S, García A and Monsalve-Serrano J. Effects of low reactivity fuel characteristics and blending ratio on low load RCCI (reactivity controlled compression ignition) performance and emissions in a heavy-duty diesel engine. Energy, Volume 90, October 2015, Pages 1261–1271.

[36] Benajes J, Molina S, García A and Monsalve-Serrano J. Effects of Direct injection timing and Blending Ratio on RCCI combustion with different Low Reactivity Fuels. Energy Conversion and Management, Volume 99, 15 July 2015, Pages 193-209.

[37] Benajes J, Pastor JV, García A and Monsalve-Serrano J. The potential of RCCI concept to meet EURO VI NOx limitation and ultra-low soot emissions in a heavy-duty engine over the whole engine map. Fuel, Volume 159, 1 November 2015, Pages 952–961.

[38] Payri R, Climent H, Salvador FJ and Favennec AG. Diesel injection system modelling. Methodology and application for a first generation common rail system. ImechE. Journal of automobile engineering. Part D, Vol 218, pp. 81-91, 2004.

[39] Payri R, Salvador FJ, Martí-Aldaraví P and Martínez-López J. Using one-dimensional modeling to analyze the influence of the use of biodiesels on the dynamic behavior of solenoid-operated injectors in common rail systems: Detailed injection system model, Energy Conversion and Management, Vol. 54, pp. 90–99, 2012.

[40] Payri R, Garcia A, Domenech V, Durrett R and Plazas A.H. An experimental study of gasoline effects on injection rate, momentum flux and spray characteristics using a common rail diesel injection system. Fuel, Vol 97, pp. 390-399, 2012.

[41] Desantes JM, Payri R, Pastor JM and Gimeno J. Experimental characterization of internal nozzle flow and diesel spray behavior. Part I: Non evaporative conditions. Atomization and Sprays, Vol. 15, pp. 489-516, 2005.

[42] Desantes JM, Pastor JV, Payri R and Pastor JM. Experimental characterization of internal nozzle flow and diesel spray behavior. Part II: Evaporative conditions. Atomization and Sprays, Vol. 15, pp. 517-543, 2005.

[43] Payri F, Olmeda P, Martín J and García A. A complete 0D thermodynamic predictive model for direct injection diesel engines. Applied Energy, Vol. 88 (12), pp. 4632-4641, 2011.

[44] Payri F, Olmeda P, Martin J and Carreño R. A New Tool to Perform Global Energy Balances in DI Diesel Engines. SAE Int. J. Engines 7(1):2014, doi:10.4271/2014-01-0665.

[45] Ma S, Zunqing Z, Liu H, Zhang Q, Yao M. Experimental investigation of the effects of diesel injection strategy on gasoline/diesel dual-fuel combustion. Applied Energy, Vol. 109, pp. 202-212, 2013.